ure of crystal quality in the epitaxial film. In the case of Au epitaxial formation on Ag(111) the growth is clearly shown to be by a Frank–van der Merwe mechanism. With these techniques we have been able to monitor the deposition of alternate layers of Au and Ag (a few monolayers at a time), observing the suppression of the surface peak of the underlying material as a measure of lattice registry. The high-energy ion scattering technique will be an important addition in studying epitaxial growth and superlattices.

We wish to acknowledge W. F. Flood for preparing the Ag samples.

[a]Present address: Solid State Division, Oak Ridge National Laboratory, Oak Ridge, Tenn. 37838.

[b]Present address: Riesterstrasse 22, A-4050 Traun, Austria.

[1]J. A. Venables and G. L. Price, in *Epitaxial Growth*, edited by J. W. Mathews (Academic, New York, 1975), part B.

[2]L. C. Feldman, P. J. Silverman, and I. Stensgaard, Nucl. Instrum. Methods 168, 589 (1980).

[3]F. Soria, J. L. Sacedon, P. M. Echenique, and D. Titterington, Surf. Sci. 68, 448 (1977).

[4]E. Bøgh, in *Channeling*, edited by D. V. Morgan (Wiley, London, 1973).

[5]I. Stensgaard, L. C. Feldman, and P. J. Silverman, Surf. Sci. 77, 513 (1978).

[6]H. J. Boehm, master's thesis, Rutgers University, 1980 (unpublished).

[7]F. Soria and J. L. Sacedon, Thin Solid Films 60, 113 (1979).

[8]H. E. Cook and J. E. Hilliard, J. Appl. Phys. 40, 2191 (1969).

[9]P. W. Palmberg and T. N. Rhodin, J. Appl. Phys. 39, 2425 (1968).

[10]C. J. Powell, Surf. Sci. 44, 29 (1974).

Phonon Focusing of Large-$\vec{k}$ Acoustic Phonons in Germanium

W. Dietsche, G. A. Northrop, and J. P. Wolfe

Physics Department and Materials Research Laboratory, University of Illinois at Urbana-Champaign, Urbana, Illinois 61801

(Received 1 June 1981)

Combining heat-pulse scanning and tunnel-junction detection, we have observed ballistic propagation of high frequency (> 700 GHz) acoustic phonons over ~1-mm path lengths in germanium. The ballistic nature of the phonons is determined by sharp variations in phonon flux with propagation angle. The phonon focusing pattern is significantly altered from that obtained with an Al bolometer (which is sensitive to longer-wavelength phonons) revealing a modification of the phonon slowness surface due to dispersion.

PACS numbers: 66.70.+f, 63.20.Dj

Over the last few years there has been a continuous effort to develop techniques for observing the ballistic propagation of phonons of ever higher frequencies over macroscopic distances.[1] Such propagation of phonons with $\vec{k}$ approaching the Brillouin-zone edge and frequencies about 1 THz has now been reported by several groups.[2-5] Large-$\vec{k}$ acoustic phonons are of particular interest because of their dispersive nature and their applicability to high-frequency phonon spectroscopy. Fundamental questions remain concerning the lifetime and mean free path of such phonons. In this Letter we report experiments which display the anisotropic propagation of large-$\vec{k}$ phonons in Ge. The ballistic phonon imaging method we describe is a general method which shows promise for producing a global picture of the acoustic-phonon dispersion in a crystal.

High-frequency phonons can be produced by a number of means, including thin-film heaters, superconducting tunnel junctions, far-infrared lasers, and hot-carrier relaxation in a semiconductor. Our experiments use this last method, with the hot carriers being photoproduced by a pulsed laser. The carrier relaxation in this case produces a broad distribution of phonon frequencies in the 1-THz range. If the ambient crystal temperature is low enough ($T \lesssim 10$ K), the mean free path of near-THz phonons should be limited by impurity, defect, or isotope scattering. In

general, the scattering is highly frequency dependent; for example, isotope (mass defect) scattering is predicted[6] to increase as ν^4. Thus, in isotopically "impure" crystals such as Ge it must be examined whether phonons of a given frequency can propagate macroscopic distances without scattering.

Experimentally a method is needed for selecting out high-frequency phonons. Other heat-pulse experiments have relied upon the reduced group velocity (and hence increased time of flight) of dispersive phonons to distinguish them from low-frequency phonons traveling at the sound velocity. However, this time selection can be subject to error, since the diffusively propagating or surface scattered low-frequency phonons also have an increased time of flight. To minimize this interference, Hu, Narayanamurti, and Chin[5] recently introduced a velocity scanning experiment which was designed to separate out the dispersive phonons from the scattered ones.

To distinguish ballistic versus diffusive propagation we examine the unique spatial properties of ballistic phonons. The underlying principle is that the ballistic phonon flux emitted from a *point source* of heat is highly anisotropic—an effect known as phonon focusing.[7] In the case of small-$\vec{k}$ phonons, striking singularities in the phonon flux have been observed in Ge for certain propagation directions.[8-10] These singularities have been traced back to lines of vanishing curvature of the constant-frequency (slowness) surface in $\vec{k}$ space. The surface normals along those zero-curvature lines correspond to group velocity directions $\vec{V}$ with mathematically infinite flux. The angular pattern of flux singularities thus provides a direct handle on the shape of the slowness surface, which for cubic crystals in the small-$\vec{k}$ limit is completely determined by the ratio of elastic constants, $C_{11}:C_{12}:C_{44}$. Until now, the calculation and observation of flux singularities has been restricted to this continuum limit.

Since the amount of frequency dispersion will in general be different for different crystal directions, the slowness surface is predicted to deform at high frequencies. This should produce changes in the phonon flux pattern. In this paper we describe heat-pulse imaging experiments in Ge which are capable of resolving the flux singularities of high-frequency dispersive phonons (> 700 GHz), and the results are compared to a model calculation parametrized with previous neutron scattering data. We will demonstrate that the singularity pattern is significantly modified even when the frequency dispersion is still rather weak. Sharp features in the spatial flux pattern can only be due to ballistically propagating phonons.[11]

To illustrate the basic ideas, we plot in Fig. 1 the constant-frequency curves for Ge in the (110) plane of phonon wave-vector space. These curves were obtained by using the semiempirical model of Zdetsis and Wang,[12] which provides a general $\omega(\vec{k})$ given the neutron-diffraction dispersion curves along symmetry axes. For the continuum limit $k \ll \pi/a$ the constant-ν curves are nonspherical as a result of the well-known elastic anisotropy of the crystal. The slowness durface *deforms* as $\vec{k}$ approaches the zone boundaries. For each different frequency an inflection point (such as the ones circled) will correspond to a different $\vec{k}$ direction and different group velocity $\vec{V}$, normal to the surface. These special group-velocity directions correspond to the real-space propagation directions of phonon-flux singularities.

To detect these singularities we employ a heat-pulse scanning method described earlier.[9] A

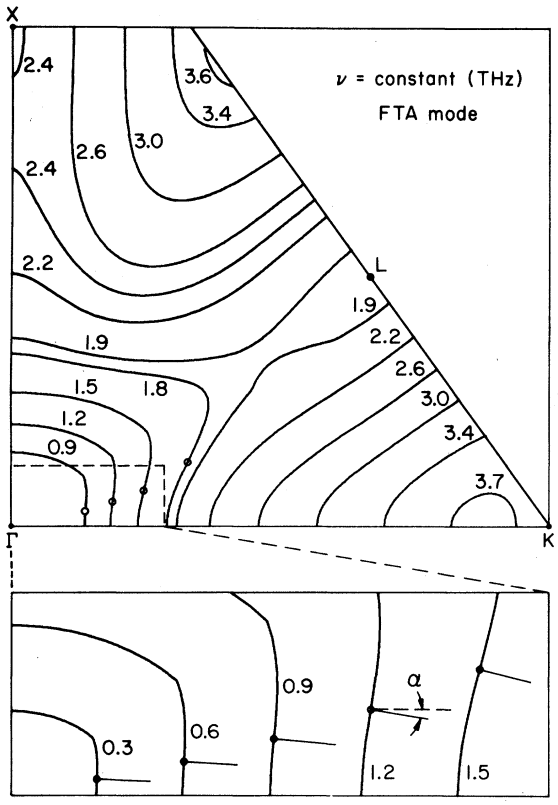

FIG. 1. Lines of constant phonon frequency in k space, shown in the (110) plane. Circles mark a few points of inflection which lead to flux singularities along the respective surface normals. The enlarged region shows how the normal directions change with frequency.

pulsed laser is slowly scanned across a (110) surface of the crystal ($T \approx 2$ K) and the arrival of the ballistic phonons is detected with a single fixed detector on the opposite face. Several significant changes have been made as follows: (a) The heat pulse is generated by direct photoexcitation of the polished Ge surface, thus producing a broad distribution of phonons by carrier thermalization. (b) Relatively thin (0.5–2 mm) samples are used to permit detection of ballistic phonons with mean free path of ~1 mm. (c) A Pb-O-Pb tunnel junction is deposited on the sample for selectively detecting phonons with frequencies above $2\Delta \approx 700$ GHz. The sensitive area of this detector is only 60×60 μm^2 for high angular resolution. For comparison with lower-ν phonons, an Al bolometer of the same size is also deposited on the crystal. (d) A microcomputer is employed to scan the laser deflection mirrors and continuously adjust the boxcar delay time to compensate for path-length variations 0.5 to 1 mm. (e) The computer adjusts the phonon intensities to account for a $\hat{n} \cdot \hat{r}/r^2$ reduction, where $\hat{n}$ is the surface normal and r the path length.[13]

With the bolometer detector we obtained sharp images at all sample thicknesses studied. For the junction detector, however, we had to reduce the sample thickness to 0.5 mm to observe sharp features in the image. This implies that phonons with frequencies above the detection threshold (700 GHz) have a smaller mean free path than lower-frequency phonons, because of scattering from the isotopes in Ge. The phonon pulses detected by the tunnel junction were considerably broader than the 60-ns laser pulse. Sharp phonon focusing features could only be observed for gate times near the onset of the arriving pulse, indicating that the later-arriving phonons were not ballistic but diffusively scattered.

Photographs of phonon flux intensity obtained with the two detectors are shown in Figs. 2(a) and 2(c). The scanning range was 110° from top to bottom, and the center of the photo corresponds to the [110] direction. The symmetry properties of the flux pattern are of course the same in both cases. A continuum-limit calculation[9] of the intersection of the flux singularities with the crystal (110) surface is shown in Fig. 2(b). Fast transverse acoustic (FTA) singularities are shown by heavy lines and slow transverse acoustic (STA) singularities by thin lines. The two diamond shapes in the top and bottom halves of the images are due to focusing close to the ⟨100⟩ directions. The four FTA "ridges" extending

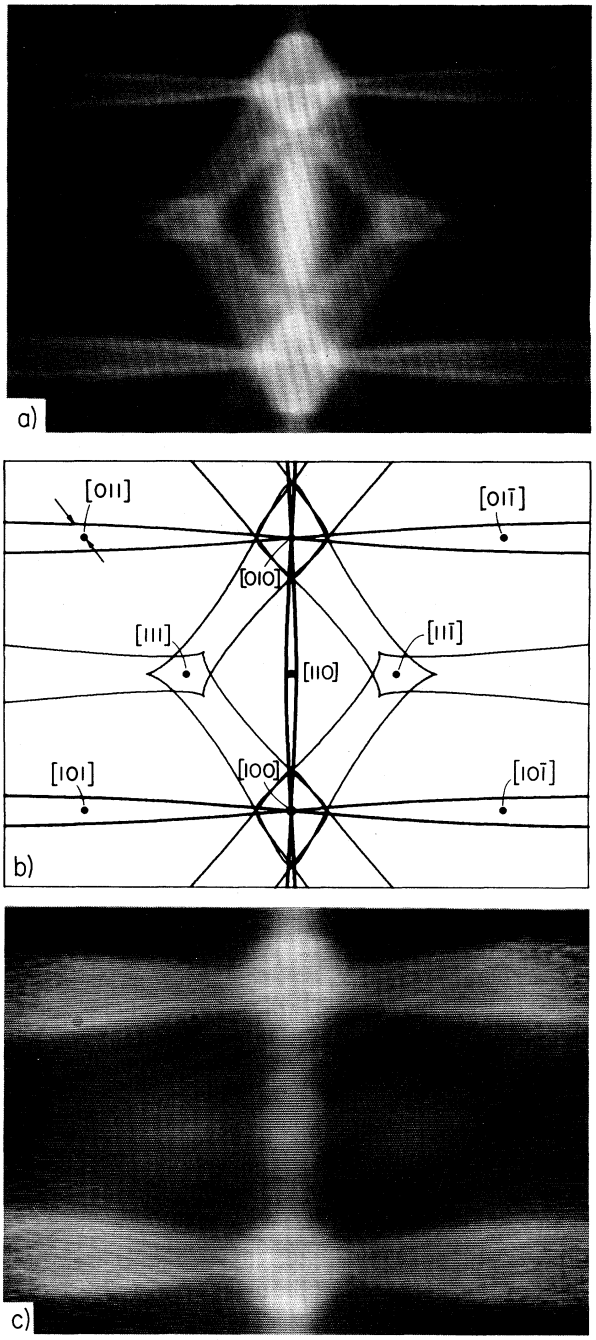

FIG. 2. Phonon images onto the (110) face. (a) Photograph of the focusing pattern obtained by the bolometer detector. (b) Phonon flux singularities calculated in the continuum (nondispersive) limit. Heavy lines are for FTA phonons, and light lines for STA phonons. The FTA ridge opening angle α, also defined in Fig. 1, is obtained from the distance between the arrows. (c) Focusing pattern obtained with the Pb tunnel-junction detector. Note that the FTA ridges, extending horizontally from the [100] and [010] directions are much wider than the ones in (a) and (b).

from each of these diamonds connect the ⟨100⟩ with the ⟨110⟩ directions. Each ridge is bounded by two singularity lines running almost parallel to the {100} planes. As anticipated, the low-frequency image [Fig. 2(a)] agrees well with these continuum-model predictions.

In contrast, the width of the FTA ridge in the tunnel-junction image [Fig. 2(c)] shows a marked deviation from the low-frequency pattern. In this high-frequency image distinguishable peaks in the intensities are observed, but they are more than twice as far apart as in the bolometer image. This difference must be due to frequency dispersion at the higher phonon frequencies detected by the tunnel junction.

There are also several qualitative differences in the two images. The shape of the STA diamond around the ⟨100⟩ axes is discernibly rounder in the high-frequency image. In addition, the STA structure extending toward the ⟨111⟩ directions is absent, possibly indicating that the STA phonons have a shorter mean free path or are reduced by dispersive effects. Indeed preliminary calculations show that the intensity of the STA phonons in the ⟨111⟩ direction may be substantially reduced at higher frequencies.[14] In this Letter we concentrate on the frequency dependence of the FTA mode, in order to obtain a semiquantitative understanding of the dispersive effects.

What is the expected shift in the singularity pattern for dispersive phonons? A calculation of the complete flux pattern is clearly more difficult than in the continuum limit. We have used the program of Zdetsis to find the constant-frequency surfaces in k space, as in Fig. 1. The singularity directions are then determined by finding $\vec{V}$ at points of vanishing Gaussian curvature on this surface, as previously described by Northrop and Wolfe.[9] We predict the FTA ridge angle α to increase with frequency as shown in Fig. 3. Thus, considering the detector response (shaded region), the ballistic-phonon–imaging measurement of α is in reasonable agreement with the calculation.

We note that the observed high-frequency pattern is considerably sharper than one might expect from the broad tunnel-junction frequency response. In fact we believe that only a narrow band of phonon frequencies are sampled in this image. The reason for this frequency selection comes from isotope scattering in Ge. Using the well-known formula for mass-defect scattering,[6] we find the phonon scattering rate $\tau^{-1} = (3.7 \times 10^{-41}\ \mathrm{s}^3)\nu^4$ for Ge, which is close to that determined

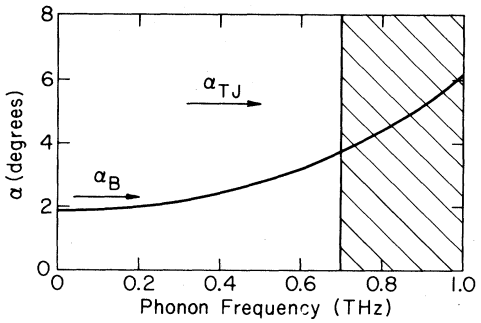

FIG. 3. Calculated frequency dependence of α, the opening angle of the FTA ridge. Arrows mark the experimental values obtained with the bolometer (α_B) and the tunnel junction (α_{TJ}). The shaded region indicates the sensitive range of the tunnel-junction detector.

from thermal conductivity.[15] For a path length of 0.5 mm the percentage of ballistically transmitted phonons is then computed to be 28% at 700 GHz and only 3% at 900 GHz. Thus in our experiment, a convolution of the frequency distribution of ballistically transmitted phonons with the detector response yields a quasimonochromatic distribution. The observed FTA singularities are consistent with our phonon-focusing calculation for this frequency distribution. In isotopically pure crystals, where high-frequency phonons are more readily transmitted, it should be possible to observe shifts in the spatial pattern by using a broadband detector and simply adjusting the time delay, i.e., group velocity. In that case the flux pattern would be calculated from the intersection of a constant-*velocity* surface with the singularity surfaces in $\vec{k}$ space.

In conclusion we have observed the ballistic propagation of dispersive phonons over ~1-mm path lengths in Ge. The focusing properties of these phonons are markedly changed from the continuum limit. In particular the FTA ridge angle was widened by a factor of 2.3. This is quite remarkable since the deviation from linear dispersion is less than 15% at 700 GHz. Clearly, from Fig. 1, the effect of dispersion on phonon focusing will be even more dramatic as one moves further towards the Brillouin-zone edge. In a practical sense, these large spatial shifts of the dispersive focusing pattern must be kept in mind when designing and evaluating experiments with large-$\vec{k}$ phonons.

We are grateful to A. D. Zdetsis for providing us with his program which generates $\omega(\vec{k})$ in Ge. This research was supported in part by the National Science Foundation under the Materials Research Laboratory Grant No. DMR-77-23999.

One of us (W.D.) acknowledges a travel grant by Deutsche Forschungsgemeinschaft.

[1]See, for example, a recent review by W. Bron, Rep. Prog. Phys. 43, 301 (1980).
[2]D. Huet, J. P. Maneval, and A. Zylberstejn, Phys. Rev. Lett. 29, 1092 (1972).
[3]W. Grill and O. Weis, Phys. Rev. Lett. 9, 588 (1975).
[4]R. G. Ulbrich, V. Narayanamurti, and M. A. Chin, Phys. Rev. Lett. 45, 1432 (1980).
[5]P. Hu, V. Narayanamurti, and M. A. Chin, Phys. Rev. Lett. 46, 192 (1981).
[6]P. G. Klemens, in *Solid State Physics*, edited by F. Seitz and D. Turnbull (Academic, New York, 1965), Vol. 7.
[7]B. Taylor, H. J. Maris, and C. Elbaum, Phys. Rev. Lett. 23, 416 (1969).
[8]J. C. Hensel and R. C. Dynes, Phys. Rev. Lett. 43, 1033 (1979).
[9]G. A. Northrop and J. P. Wolfe, Phys. Rev. Lett. 43, 1424 (1979), and Phys. Rev. B 22, 6169 (1980).
[10]W. Eisenmenger, in *Proceedings of the Third International Conference on Phonon Scattering in Condensed Matter, Providence, Rhode Island, 1979*, edited by H. J. Maris (Plenum, New York, 1980), p. 303.
[11]How does scattering affect the pattern? It should be similar to viewing a sharp optical image through fog: A weak but sharp image remains, superimposed on a smooth background.
[12]A. D. Zdetsis and C. S. Wang, Phys. Rev. B 19, 2999 (1979); A. D. Zdetsis, in *Proceedings of the International Conference on Lattice Dynamics, Paris, 1977*, edited by M. Balkanski (Flammarion, Paris, 1978) p. 45, inelastic neutron scattering data, and references herein.
[13]We did not, however, compensate for the intensity reduction by scattering.
[14]G. Northrop, to be published.
[15]J. Callaway, Phys. Rev. 113, 1046 (1959).

Nematic–Smectic-*A*–Smectic-*C* Multicritical Point

R. DeHoff, R. Biggers, D. Brisbin, R. Mahmood, C. Gooden, and D. L. Johnson
Department of Physics, Kent State University, Kent, Ohio 44242
(Received 5 March 1981)

A study of the phase diagram near the nematic–smectic-*A*–smectic-*C* multicritical point and of nematic–smectic-*C* transition entropies leads to the conclusion that this is not a Lifshitz point. It is shown that a biaxial second-rank tensor order parameter may be needed.

PACS numbers: 64.70.Ew, 64.60.Kw

When the nematic–smectic-*A*–smectic *C* (NAC) multicritical point was first suggested, the two proposed explanations of it were very different. Chu and McMillan[1] (CM) proposed a model in which smectic-*C* has the dipolar order parameter of McMillan's theory,[2] while the smectic-*A* order parameter was the one-dimensional density wave of Kobayashi,[3] McMillan,[4] and deGennes.[5] Tilt of the director away from the layer normal entered the model somewhat incidentally through a gradient term coupling the two order parameters. Chen and Lubensky[6] (CL) found an NAC point in a model where the only order parameter was the one-dimensional density wave. Tilt of the director relative to the layer normal is a central feature of the model and occurs when the coefficient of the transverse gradient term becomes negative. From the experimental point of view the differences between the two models are primarily twofold. First, in the CL model the NAC point is a type of Lifshitz point,[7] which leads to the prediction that x-ray scattering in the nematic phase near the NAC point falls off in the transverse direction as $k_\perp^{-4}$, rather than the usual $k_\perp^{-2}$ predicted by the CM model. Secondly, the nematic–smectic-*C* (NC) transition entropy is zero in the CM model but finite in the CL model because of the Brazovskii[8-10] effect. The NC entropy was found to be finite when the NAC point was discovered experimentally.[11]

In this Letter evidence is presented, based on the topology of the phase diagram and the nematic–smectic-*C* transition entropy, that for the system studied, which is the same as the one studied previously,[11] the NAC point is likely not either of the above kinds of multicritical points. Instead it conforms well with a phenomenological Landau expansion suggested recently by Benguigui,[12] for which is offered a physical interpretation.

In earlier work on mixtures of octyl- and heptyloxy-*p'*-pentylphenyl thiolbenzoate ($\overline{7}S5$-$\overline{8}S5$),[11] gross features of the phase diagram were deter-

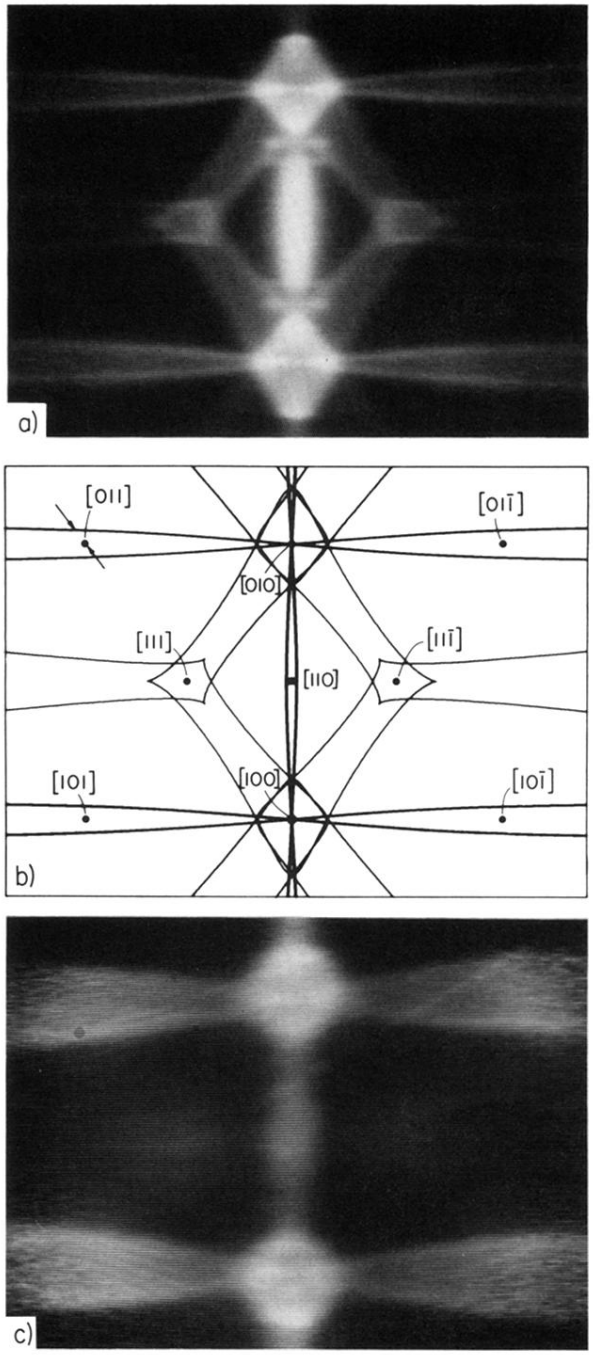

FIG. 2. Phonon images onto the (110) face. (a) Photograph of the focusing pattern obtained by the bolometer detector. (b) Phonon flux singularities calculated in the continuum (nondispersive) limit. Heavy lines are for FTA phonons, and light lines for STA phonons. The FTA ridge opening angle α, also defined in Fig. 1, is obtained from the distance between the arrows. (c) Focusing pattern obtained with the Pb tunnel-junction detector. Note that the FTA ridges, extending horizontally from the [100] and [010] directions are much wider than the ones in (a) and (b).